HHS Public Access

Author manuscript

FEBS Lett. Author manuscript; available in PMC 2018 April 01.

Published in final edited form as:

FEBS Lett. 2017 April ; 591(7): 1018–1028. doi:10.1002/1873-3468.12610.

Sortilin 1 knockout alters basal adipose glucose metabolism but not diet-induced obesity in mice

Jibiao Li, **David J. Matye**, **Yifeng Wang**, and **Tiangang Li***

Department of Pharmacology, Toxicology and Therapeutics, University of Kansas Medical Center, Kansas City, Kansas 66160

Abstract

Sortilin 1 (Sort1) is a trafficking receptor that has been implicated in the regulation of plasma cholesterol in humans and mice. Here, we use metabolomics and hyperinsulinemic-euglycemic clamp approaches to obtain further understanding of the *in vivo* effects of *Sort1* deletion on diet-induced obesity as well as on adipose lipid and glucose metabolism. Results show that *Sort1* knockout does not affect Western diet-induced obesity or adipose fatty acid and ceramide concentrations. Under the basal fasting state, chow-fed *Sort1* knockout mice have decreased adipose glycolytic metabolites, but *Sort1* deletion does not affect insulin-stimulated tissue glucose uptake during the insulin clamp. These results suggest that *Sort1* loss-of-function *in vivo* does not affect obesity development, but differentially modulates adipose glucose metabolism under fasting and insulin-stimulated states.

Keywords

Obesity; diabetes; hyperlipidemia; cholesterol

Introduction

Sortilin 1 (Sort1) is one of the several vacuolar protein sorting 10 protein (VPS10P)-domain receptors. The VPS10P-domain receptors are single transmembrane receptors that bind various functionally–unrelated proteins and mediate their intracellular vesicular trafficking to the endocytic pathway either from the trans-Golgi apparatus or after endocytosis (1). Recent genome-wide association studies (GWAS) revealed that *SORT1* gene was strongly associated with plasma low-density lipoprotein cholesterol concentrations and the risk of cardiovascular disease in large human populations (2, 3). In experimental models, hepatic Sort1 has been shown to modulate hepatic VLDL production and plasma lipoprotein clearance (4–10). Furthermore, *Sort1* knockout mice showed reduced atherosclerosis, which may be attributed to attenuated macrophage activation (11, 12) and vascular calcification (13).

*Corresponding author: Tiangang Li, PhD., Department of Pharmacology, Toxicology and Therapeutics, The University of Kansas Medical Center, 3901 Rainbow Blvd, Kansas City, KS 66160, Phone: 913-588-9974, Fax: 913-588-7501, tli@kumc.edu.

Author Contribution. Jibiao Li, David J. Matye and Yifeng Wang designed and performed research, and analyzed data. Tiangang Li designed research, analyzed data and wrote the paper. These authors declare no conflict of interest.

Sort1 is highly expressed in adipocytes. Previous studies identified Sort1 as an essential component of the GLUT4 storage vesicle (GSV) (14, 15). The N-terminal luminal domain of Sort1 interacts with Glut4, while the cytoplasmic tail of Sort1 interacts with adaptor proteins to facilitate GSV formation (16–21). It has been shown in both adipocytes and myocytes that Sort1 was required for insulin-dependent glucose uptake (20, 22–24). However, no studies so far have investigated the *in vivo* impact of Sort1 deficiency on glucose metabolism in fat tissues. Paradoxically, a more recent study showed that *Sort1* KO mice were protected against high fat diet-induced obesity and showed improved insulin sensitivity in an insulin tolerance test, which was partially attributed to lower acid sphingomyelinase (aSMase) activity in the liver and the adipose tissue (25). Because obesity and adipose lipid and glucose metabolism profoundly impact hepatic lipid production and plasma lipid concentration, there is a clear need to clarify the role of Sort1 in the regulation of obesity and adipose lipid and glucose metabolism under physiological and pathological settings *in vivo*. Such knowledge is needed to improve current understanding of the novel role of Sort1 in the regulation of lipid metabolism and inflammation in health and disease processes.

In this study, we investigated the impact of Sort1 loss-of-function on obesity, adipose lipid and glucose metabolism by using metabolite analysis and hyperinsulinemic-euglycemic clamp study. Findings from this study showed that *Sort1* KO mice had decreased adipose glycolytic metabolites at basal fasting state. However, Sort1 deficiency did not affect Western diet-induced obesity and adipose fatty acid and sphingolipid concentration, and had no significant effect on insulin-stimulated tissue glucose uptake during the hyperinsulinemic-euglycemic clamp study under either chow-fed condition or after diet-induced obesity.

Materials and Methods

Reagents

The antibodies against Sort1 (ab16640; Lot: GR64653-1), Glut4 (ab654; Lot: GR101575-1) and α-Tubulin (ab7291; Lot: GR122217-1) were purchased from Abcam (Cambridge, MA). The antibody against Histone 3 (9717; Lot: 8) was purchased from Cell Signaling Technology (Danvers, MA). The antibody against Actin (A5441; Lot: 063M4808) was purchased from Sigma (St. Louis, MO).

Mice

Global *Sort1* KO mice were purchased from Taconic Biosciences Inc. as described previously (10). The *Sort1* gene was silenced by gene trapping technology that inserted a stop codon into the second intron of the *Sort1* gene. Mice were obtained on mixed background (129/SvEv/C57BL/6) and were backcrossed to C57BL/6J (The Jackson Lab) for multiple generations. Male F7 and F8 generations of *Sort1* KO and WT littermates were used for this study. Western diet feeding was initiated when mice were 10 weeks of age. All mice were maintained on a standard chow diet and water *ad libitum*. The Western diet (TD. 88137, Harlan Teklad) contains 21% milk fat (w/w) and 0.2% cholesterol. All animal protocols were approved by the Institutional Animal Care and Use Committee.

Western blot

Tissue homogenates were prepared in 1X RIPA buffer containing 1% SDS and protease inhibitor cocktail, and was incubated for 1 h on ice, followed by brief sonication. Protein concentrations were determined by a BCA assay kit (Rockford, IL). A representing blot is shown. Relative band intensity (normalized to loading controls) was determined by ImageJ software. Average band intensity was expressed as mean ± S.E.M..

Glucose tolerance test

Mice were fasted overnight and received a single intra-peritoneal injection of glucose at 2g/kg body weight. A drop of blood was collected from the tail and glucose was measured with a glucose monitor.

Analysis of tissue metabolites

This was performed by Metabolon Inc (Durham, NC). Several recovery standards were added based on tissue weight prior to sample extraction for quality control and data normalization. Extract was analyzed on four UPLC-MS/MS systems, utilizing: 1) positive ion mode, early elution; 2) positive ion mode, late elution; 3) negative ion mode and 4) polar-negative ion mode. All methods utilized a Waters ACQUITY UPLC and a Thermo Scientific Q-Exactive high resolution/accurate mass spectrometer interfaced with a heated electrospray ionization (HESI-II) source and Orbitrap mass analyzer operated at 35,000 mass resolution. Peaks were quantified using area-under-the-curve. Two-way ANOVA and t-test were used for statistical analysis.

Hyperinsulinemic-euglycemic clamp

Insulin clamps were performed at the Mouse Metabolic Phenotyping Center (MMPC) at the Vanderbilt University. Mice were maintained on chow or Western diet for 8 weeks. Catheters were implanted into a carotid artery and a jugular vein for sampling and infusions respectively five days before the study. The study was initiated in mice after fasting for 5 h. [3-^{3}H]-glucose was continuously infused at 0.075 μCi/min for a 90 min equilibration and basal sampling period. [3-^{3}H]-glucose was mixed with the non-radioactive glucose infusate (infusate specific activity of 0.5 μCi/mg glucose) during the 2 h clamp period. Arterial glucose was clamped using a variable rate of glucose infusion. Baseline plasma variables were calculated as the mean of values obtained in blood samples collected at 15 and 5 min prior insulin infusion (2.5 mU/Kg/min for chow-fed mice or 4 mU/kg/min for Western diet-fed mice). Blood was taken from 80–120 min for the determination of [3-^{3}H]-glucose. Clamp insulin was determined at 100 min and 120 min. At 120 min, an intravenous bolus of 13 μCi 2-[^{14}C]-deoxyglucose was administered. Blood was taken from 2–25min for determination of 2-[^{14}C]-deoxyglucose. After the last sample, mice were anesthetized. Plasma insulin and c-peptide were determined by RIA. Radioactivity of [3-^{3}H]-glucose, 2-[^{14}C]-deoxyglucose and 2-[^{14}C]-deoxyglucose -6-phosphate in plasma or tissues were determined by liquid scintillation counting. Glucose appearance (Ra) and disappearance (Rd) rates were determined using steady-state equations (26). Endogenous glucose appearance (endoRa) was determined by subtracting the glucose infusion rate (GIR) from total Ra. The glucose metabolic index (Rg) was calculated as previously described (27).

Statistical analysis

Results were expressed as mean ± S.E.M.. Statistical analysis was performed by Student's t-test or ANOVA. A $p < 0.05$ was considered statistically significant.

Results

Sortilin 1 knockout did not affect Western diet-induced obesity, adipose fatty acid and sphingolipid metabolism

To investigate the role of Sort1 on diet-induced obesity, we fed WT and *Sort1* KO mice a chow or a Western diet. We found that WT mice and *Sort1* KO mice gained similar amount of body weight over the 8-week feeding period (Fig 1A). Glucose tolerance test also did not show significant difference in glucose tolerance between WT and *Sort1* KO mice on either chow diet or Western diet (Fig 1B). These results are inconsistent with a recent study reporting that high fat diet-fed *Sort1* KO mice showed lower body weight and decreased adipose aSMase enzyme activity (25). Ceramide signaling contributes to insulin resistance and impaired tissue glucose metabolism in obesity (28, 29). A previous *in vitro* study showed that Sort1 played a redundant role in addition to the mannose 6-phosphate receptor (M6PR) in mediating the lysosomal trafficking of aSMase that hydrolyzes sphingomyelins to ceramides (30). Thus it is thought that Sort1 deficiency may decrease the aSMase-mediated ceramide production in lysosomes. Here we showed that the relative concentrations of C16:0-ceramide, the principle ceramide species mediating the development of insulin resistance and obesity (28, 29), and its precursor C16:0 sphingomyelin were not different between *Sort1* KO mice and WT controls under either chow-fed or Western diet-fed conditions (Fig 1C).

Sortilin 1 knockout decreased glycolytic metabolites in adipose tissue under chow-fed fasting condition

We next studied the impact of Sort1 loss-of-function on adipose glucose metabolism in mice. Consistent with a previous report (24), Western diet feeding decreased adipose Sort1 protein (Fig 2A). However, muscle Sort1 protein was not altered in Western diet-fed mice (Fig 2B). Glut4 protein was reduced in white adipose tissue but not muscle of Western diet-fed WT mice (Fig 2A, 2B), which was a known phenomenon (31). WT and *Sort1* KO mice showed similar Glut4 protein levels in adipose and skeletal muscle (Fig 2A, 2B), suggesting that Sort1 loss-of-function did not affect Glut4 protein abundance *in vivo*.

Next, we measured the relative concentrations of glycolytic metabolites in the adipose of overnight fasted mice, which may reflect basal glucose metabolism under non-insulin stimulated state. Chow-fed *Sort1* KO mice showed significantly reduced relative concentrations of glucose and all detected glycolytic intermediates except lactate (Fig 2C). Such changes closely mimicked the significantly decreased adipose glycolytic metabolites in Western diet-fed WT mice (Fig 2C), which was in line with impaired adipose glucose uptake in obesity. After Western diet feeding, WT and *Sort1* KO mice no longer showed differential levels of glucose and glycolytic intermediates (Fig 2C), which could be due to the predominant reduction of the glycolytic metabolites caused by Western diet-induced obesity. To seek further evidence of reduced basal glycolysis in adipose of *Sort1* KO mice, we

measured the relative concentrations of the TCA cycle intermediates since the end glycolytic metabolite is a substrate for TCA cycle. Results in Fig 2D showed that the relative concentration of citrate, the product of the first reaction in the TCA cycle, was reduced by ~70% in chow-fed *Sort1* KO mice compared to WT. In addition, the relative concentrations of several downstream TCA cycle intermediates aconitate, α-ketoglutarate and fumarate were also significantly decreased in chow-fed *Sort1* KO mice (Fig 2D). Western diet feeding resulted in more reduction of citrate, aconitate, fumarate and malate in both WT and *Sort1* KO mice (Fig 2D), which suggested that obesity was associated with decreased TCA cycle metabolites in the adipose tissues.

Altered cellular glycolysis may also affect fatty acid metabolism in the adipose tissues. However, no genotype-dependent differences in the relative concentrations of long-chain fatty acids, glycerol, monoacylglycerol (MAG) and diacylglycerol (DAG) were observed between WT and *Sort1* KO mice under chow-fed or Western diet-fed conditions (Fig 3A, 3C). On the other hand, glycerol 3-phosphate, a significant amount of which is derived from glycolysis, was reduced in chow-fed *Sort1* KO mice and also in Western diet-fed WT and *Sort1* KO mice (Fig 3C). It is worth noting that Western diet significantly decreased ketone body 3-hydroxylbutyrate but increased other 3-hydroxy fatty acid species in WT mice (Fig 3B), which, in the absence of increased fatty acids, indicated impaired mitochondria fatty acid oxidation. Species of 3-hydroxy fatty acids and ketone body 3-hydroxybutyrate were not different between chow-fed WT and *Sort1* KO mice (Fig 3B). These results suggest that, despite altered glycolytic activity, Sort1-deficiency did not affect adipose fatty acid metabolism. In addition, Western diet feeding strongly and consistently decreased major C16 and C18 long chain fatty acids as well as MAG, DAG and glycerol to similar levels in WT and *Sort1* KO mice (Fig 3A, 3C), which may reflect a metabolic shift to increased triglyceride synthesis and fat storage as an adaptive response to higher dietary fat intake.

Sort1 deficiency did not affect insulin-stimulated glucose uptake during insulin clamp in mice

Next, hyperinsulinemic-euglycemic clamp was used to further determine the effects of Sort1 loss-of-function on *in vivo* insulin action and tissue-specific glucose handling in mice. During the clamp, the total glucose infusion rate was similar between chow-fed WT and *Sort1* KO mice (Fig 4A, 4B). The endogenous glucose production (EndoRa) was similar between WT and *Sort1* KO mice (Fig 4C). The insulin-stimulated glucose uptake into muscle and white and brown adipose tissues was not different between WT and *Sort1* KO mice (Fig 4D). Interestingly, despite well-maintained euglycemia during the clamp (Fig 4A), the clamp insulin levels were significantly lower in *Sort1* KO mice (Fig 4F). During the insulin clamp, the plasma insulin represented the mixture of exogenously infused insulin and endogenously secreted insulin by the β cells. Fig 4G showed that plasma C-peptide during clamp was also significantly reduced in *Sort1* KO mice, suggesting lower clamp insulin was likely due to decreased endogenous insulin secretion but not increased liver insulin clearance in *Sort1* KO mice. The endogenous insulin production in the presence of exogenous glucose and insulin infusion during insulin clamp is still a poorly understood process. The underlying cause of decreased clamp insulin in chow-fed *Sort1* KO mice still requires further investigation. In Western diet-fed mice, the clamp glucose was well maintained and

the clamp insulin levels were similar in WT and *Sort1* KO mice (Fig 5A, 5B). Under these conditions, *Sort1* KO mice and WT mice exhibited similar total glucose infusion rate (GIR) (Fig 5C). Insulin-stimulated tissue glucose uptake into the muscle and white and brown fat were similar between the groups (Fig 5D). Total glucose flux (Rd) and endogenous glucose production (endoRa) were also similar between the two groups (Fig 5E, 5F).

Discussion

This study characterized the impact of Sort1 loss-of-function on adipose glucose metabolism in mouse models. Such *in vivo* studies are currently lacking in the field but are clearly needed to better define the pathophysiological function of Sort1 and its implication in the pathogenesis of obesity and diabetes. Our studies showed that Sort1 loss-of-function differentially affected adipose glucose metabolism under basal fasting state and insulin-stimulated state. By studying the *in vivo* insulin action and insulin-stimulated organ-specific glucose uptake with hyperinsulinemic-euglycemic clamp, we found that chow-fed *Sort1* KO mice generally showed normal overall glucose flux and tissue glucose uptake during insulin clamp, suggesting that, at least under the clamp condition, Sort1 deficiency did not significantly impair insulin – stimulated glucose uptake into muscle and adipose. If lower clamp insulin is taken into consideration, the overall insulin sensitivity may be actually slightly higher in *Sort1* KO mice. The adipose and muscle Glut4 protein abundance was also similar between *Sort1* KO mice and WT. This is different from genetic deletion of another key GSV component insulin-regulated aminopeptidase (IRAP) in mice, which resulted in decreased Glut4 protein abundance in muscle and adipose (32). Similarly, deletion of the GSV component low density lipoprotein receptor – related protein 1 (LRP1) in adipose tissue also reduced adipose Glut4 protein abundance in mice (33). Given that Sort1 knockdown reduced Glut4 protein abundance and impaired insulin-dependent glucose uptake in cultured adipocytes, a more plausible explanation may be that the congenital loss of Sort1 function *in vivo* can be compensated by other GSV components. In addition to IRAP and LRP1, M6PR and sorting-related receptor with type-A repeats (SorLA) were identified as components of purified GSVs from rat adipocytes (33, 34). M6PR, SorLA and LRP1 can also interact with and recruit the Golgi-localized γ-ear-containing Arf-binding proteins (GGA) of coat adaptor proteins that are required for intracellular vesicle trafficking (35). The existence of such functional redundancy is possible as loss of insulin-dependent glucose uptake may be detrimental to many cell types.

In contrast to insulin-stimulated glucose uptake, we found consistently decreased glycolytic and TCA cycle intermediate metabolites in the adipose of chow-fed fasted *Sort1* KO mice. The altered glycolytic and TCA cycle metabolite profile closely resembled the changes caused by Western diet feeding to WT mice, which was expected to cause adipose insulin resistance that impaired cellular glucose uptake and metabolism. These genotype-dependent changes of glycolytic metabolites under chow-fed conditions thus suggest that there is a causal link between Sort1 deficiency and decreased glucose metabolism in the adipose tissue. Under fasting, adipocytes are exposed to relatively lower concentrations of circulating insulin. Since chow-fed WT and *Sort1* KO mice had similar adipose GLUT4 protein, reduced glycolytic intermediates in chow-fed *Sort1* KO mice could be a result of reduced GLUT4 membrane translocation, which would be consistent with the required role of Sort1

in conferring the insulin responsiveness of GSV demonstrated in cultured adipocytes (20, 22). However, such changes may have been masked after strong exogenous insulin stimulation during the insulin clamp. Reduced basal glucose uptake has also been reported in adipocytes isolated from mice lacking another GSV component IRAP ex vivo (32). It was not surprising to see that *Sort1* KO mice had normal fasting glucose levels, because both mice lacking Glut4 and mice lacking IRAP generally maintained normal glycaemia (32, 36). When fed a Western diet, Sort1 deficiency did not further decrease adipose glycolytic metabolites. One possible explanation may be that Western diet-induced obesity may have a much stronger effect in decreasing adipose glucose metabolism, which therefore masked the genotype-dependent effects in Western diet-fed WT and *Sort1* KO mice.

In our study, Sort1 deficiency did not affect Western diet-induced weight gain. This finding is inconsistent with a previous study showing that *Sort1* KO mice were resistant to high fat diet-induced obesity (25). This study showed that high fat diet-fed *Sort1* KO mice had lower adipose aSMase activity than high fat diet-fed WT mice, but adipose ceramide concentrations were not directly quantified (25). Cellular ceramides can be produced through other aSMase-independent pathways. Our metabolite analysis revealed no difference in ceramide levels between WT and *Sort1* KO mice on either chow diet or Western diet. Unfortunately, the study did not report the adipose aSMase activity in mice under the chow-fed condition without body weight difference between the two groups (25), which would be more informative because obesity is known to increase aSMase activity (37). Although the underlying cause of such discrepancy is still not clear, we would like to note that the *Sort1* KO mice used in the two studies were generated independently with different targeting strategies (10, 38). In addition, the fat-enriched diets used in the two studies were different. The previous study used a diet contained 60% fat calories from lard (25), while the Western diet used in our study contained 42% fat calories from milk fat. Therefore we cannot rule out the possibility that the fat content or the source of dietary fat may potentially influence the obesity phenotypes in *Sort1* KO mice and WT controls. To our knowledge, there have been no other independent studies reporting the effect of Sort1 ablation on diet-induced weight gain in mice. A few previous studies have employed high fat diet feeding to *Sort1* KO mice on *Ldlr*−/−, *ApoE*−/− or *Apobec1*−/−/*hAPOB-tg* genetic background (4, 11–13). However, these studies did not report data on weight gain in these mice. Obesity, adipocyte dysfunction and insulin resistance are early events associated with obesity development, which critically contributes to the pathogenesis of hepatic steatosis and hyperlipidemia. Determining whether adipose Sort1 deficiency affects obesity development and adipose lipid and glucose metabolism is important in improving our understanding of the mechanistic link between Sort1 function and plasma lipid concentrations.

Acknowledgments

This work is supported in part by the American Diabetes Association Junior Faculty Award (T.L.), NIH grant 1R01DK102487-01 (T.L), and the NIGMS grants P20GM103549 and P30GM118247.

Abbreviations

Sort1 Sortilin 1

VPS10P	vacuolar protein sorting 10 protein
aSMase	acid sphingomyelinase
SorLA	sorting-related receptor with type-A repeats
GSV	Glut4 storage vesicles
KO	knockout
GIR	glucose infusion rate
MAG	monoacylglycerol
DAG	diacylglycerol
IRAP	insulin-regulated aminopeptidase
LRP1	low density lipoprotein receptor – related protein 1
M6PR	mannose 6-phosphate receptor
GGA	Golgi-localized γ-ear-containing Arf-binding proteins

References

1. Hermey G. The Vps10p-domain receptor family. Cell Mol Life Sci. 2009; 66:2677–2689. [PubMed: 19434368]
2. Kathiresan S, Melander O, Guiducci C, Surti A, Burtt NP, Rieder MJ, Cooper GM, Roos C, Voight BF, Havulinna AS, Wahlstrand B, Hedner T, Corella D, Tai ES, Ordovas JM, Berglund G, Vartiainen E, Jousilahti P, Hedblad B, Taskinen MR, Newton-Cheh C, Salomaa V, Peltonen L, Groop L, Altshuler DM, Orho-Melander M. Six new loci associated with blood low-density lipoprotein cholesterol, high-density lipoprotein cholesterol or triglycerides in humans. Nat Genet. 2008; 40:189–197. [PubMed: 18193044]
3. Kathiresan S, Voight BF, Purcell S, Musunuru K, Ardissino D, Mannucci PM, Anand S, Engert JC, Samani NJ, Schunkert H, Erdmann J, Reilly MP, Rader DJ, Morgan T, Spertus JA, Stoll M, Girelli D, McKeown PP, Patterson CC, Siscovick DS, O'Donnell CJ, Elosua R, Peltonen L, Salomaa V, Schwartz SM, Melander O, Altshuler D, Ardissino D, Merlini PA, Berzuini C, Bernardinelli L, Peyvandi F, Tubaro M, Celli P, Ferrario M, Fetiveau R, Marziliano N, Casari G, Galli M, Ribichini F, Rossi M, Bernardi F, Zonzin P, Piazza A, Mannucci PM, Schwartz SM, Siscovick DS, Yee J, Friedlander Y, Elosua R, Marrugat J, Lucas G, Subirana I, Sala J, Ramos R, Kathiresan S, Meigs JB, Williams G, Nathan DM, MacRae CA, O'Donnell CJ, Salomaa V, Havulinna AS, Peltonen L, Melander O, Berglund G, Voight BF, Kathiresan S, Hirschhorn JN, Asselta R, Duga S, Spreafico M, Musunuru K, Daly MJ, Purcell S, Voight BF, Purcell S, Nemesh J, Korn JM, McCarroll SA, Schwartz SM, Yee J, Kathiresan S, Lucas G, Subirana I, Elosua R, Surti A, Guiducci C, Gianniny L, Mirel D, Parkin M, Burtt N, Gabriel SB, Samani NJ, Thompson JR, Braund PS, Wright BJ, Balmforth AJ, Ball SG, Hall A, Schunkert H, Erdmann J, Linsel-Nitschke P, Lieb W, Ziegler A, Konig I, Hengstenberg C, Fischer M, Stark K, Grosshennig A, Preuss M, Wichmann HE, Schreiber S, Schunkert H, Samani NJ, Erdmann J, Ouwehand W, Hengstenberg C, Deloukas P, Scholz M, Cambien F, Reilly MP, Li M, Chen Z, Wilensky R, Matthai W, Qasim A, Hakonarson HH, Devaney J, Burnett MS, Pichard AD, Kent KM, Satler L, Lindsay JM, Waksman R, Knouff CW, Waterworth DM, Walker MC, Mooser V, Epstein SE, Rader DJ, Scheffold T, Berger K, Stoll M, Huge A, Girelli D, Martinelli N, Olivieri O, Corrocher R, Morgan T, Spertus JA, McKeown P, Patterson CC, Schunkert H, Erdmann E, Linsel-Nitschke P, Lieb W, Ziegler A, Konig IR, Hengstenberg C, Fischer M, Stark K, Grosshennig A, Preuss M, Wichmann HE, Schreiber S, Holm H, Thorleifsson G, Thorsteinsdottir U, Stefansson K, Engert JC, Do R, Xie C, Anand S, Kathiresan S, Ardissino D,

Mannucci PM, Siscovick D, O'Donnell CJ, Samani NJ, Melander O, Elosua R, Peltonen L, Salomaa V, Schwartz SM, Altshuler D. Myocardial Infarction Genetics C; Wellcome Trust Case Control C. Genome-wide association of early-onset myocardial infarction with single nucleotide polymorphisms and copy number variants. Nat Genet. 2009; 41:334–341. [PubMed: 19198609]

4. Kjolby M, Andersen OM, Breiderhoff T, Fjorback AW, Pedersen KM, Madsen P, Jansen P, Heeren J, Willnow TE, Nykjaer A. Sort1, encoded by the cardiovascular risk locus 1p13.3, is a regulator of hepatic lipoprotein export. Cell Metab. 2010; 12:213–223. [PubMed: 20816088]
5. Musunuru K, Strong A, Frank-Kamenetsky M, Lee NE, Ahfeldt T, Sachs KV, Li X, Li H, Kuperwasser N, Ruda VM, Pirruccello JP, Muchmore B, Prokunina-Olsson L, Hall JL, Schadt EE, Morales CR, Lund-Katz S, Phillips MC, Wong J, Cantley W, Racie T, Ejebe KG, Orho-Melander M, Melander O, Koteliansky V, Fitzgerald K, Krauss RM, Cowan CA, Kathiresan S, Rader DJ. From noncoding variant to phenotype via SORT1 at the 1p13 cholesterol locus. Nature. 2010; 466:714–719. [PubMed: 20686566]
6. Gustafsen C, Kjolby M, Nyegaard M, Mattheisen M, Lundhede J, Buttenschon H, Mors O, Bentzon JF, Madsen P, Nykjaer A, Glerup S. The hypercholesterolemia-risk gene SORT1 facilitates PCSK9 secretion. Cell Metab. 2014; 19:310–318. [PubMed: 24506872]
7. Butkinaree C, Canuel M, Essalmani R, Poirier S, Benjannet S, Asselin MC, Roubtsova A, Hamelin J, Marcinkiewicz J, Chamberland A, Guillemot J, Mayer G, Sisodia SS, Jacob Y, Prat A, Seidah NG. Amyloid precursor-like protein 2 and sortilin do not regulate the PCSK9 convertase-mediated low density lipoprotein receptor degradation but interact with each other. J Biol Chem. 2015
8. Li J, Bi L, Hulke M, Li T. Fish oil and fenofibrate prevented phosphorylation-dependent hepatic sortilin 1 degradation in Western diet-fed mice. J Biol Chem. 2014; 289:22437–22449. [PubMed: 24986865]
9. Bi L, Chiang JY, Ding WX, Dunn W, Roberts B, Li T. Saturated fatty acids activate ERK signaling to downregulate hepatic sortilin 1 in obese and diabetic mice. J Lipid Res. 2013; 54:2754–2762. [PubMed: 23904453]
10. Li J, Wang Y, Matye DJ, Chavan H, Krishnamurthy P, Li F, Li T. Sortilin 1 Modulates Hepatic Cholesterol Lipotoxicity in Mice via Functional Interaction with Liver Carboxylesterase 1. The Journal of biological chemistry. 2017; 292:146–160. [PubMed: 27881673]
11. Mortensen MB, Kjolby M, Gunnersen S, Larsen JV, Palmfeldt J, Falk E, Nykjaer A, Bentzon JF. Targeting sortilin in immune cells reduces proinflammatory cytokines and atherosclerosis. J Clin Invest. 2014; 124:5317–5322. [PubMed: 25401472]
12. Patel KM, Strong A, Tohyama J, Jin X, Morales CR, Billheimer J, Millar J, Kruth H, Rader DJ. Macrophage sortilin promotes LDL uptake, foam cell formation, and atherosclerosis. Circ Res. 2015; 116:789–796. [PubMed: 25593281]
13. Goettsch C, Hutcheson JD, Aikawa M, Iwata H, Pham T, Nykjaer A, Kjolby M, Rogers M, Michel T, Shibasaki M, Hagita S, Kramann R, Rader DJ, Libby P, Singh SA, Aikawa E. Sortilin mediates vascular calcification via its recruitment into extracellular vesicles. J Clin Invest. 2016
14. Lin BZ, Pilch PF, Kandror KV. Sortilin is a major protein component of Glut4-containing vesicles. The Journal of biological chemistry. 1997; 272:24145–24147. [PubMed: 9305862]
15. Morris NJ, Ross SA, Lane WS, Moestrup SK, Petersen CM, Keller SR, Lienhard GE. Sortilin is the major 110-kDa protein in GLUT4 vesicles from adipocytes. J Biol Chem. 1998; 273:3582–3587. [PubMed: 9452485]
16. Zhu Y, Doray B, Poussu A, Lehto VP, Kornfeld S. Binding of GGA2 to the lysosomal enzyme sorting motif of the mannose 6-phosphate receptor. Science. 2001; 292:1716–1718. [PubMed: 11387476]
17. Nielsen MS, Madsen P, Christensen EI, Nykjaer A, Gliemann J, Kasper D, Pohlmann R, Petersen CM. The sortilin cytoplasmic tail conveys Golgi-endosome transport and binds the VHS domain of the GGA2 sorting protein. EMBO J. 2001; 20:2180–2190. [PubMed: 11331584]
18. Kato Y, Misra S, Puertollano R, Hurley JH, Bonifacino JS. Phosphoregulation of sorting signal-VHS domain interactions by a direct electrostatic mechanism. Nature structural biology. 2002; 9:532–536. [PubMed: 12032548]
19. Pilch PF. The mass action hypothesis: formation of Glut4 storage vesicles, a tissue-specific, regulated exocytic compartment. Acta physiologica. 2008; 192:89–101. [PubMed: 18171432]

20. Shi J, Kandror KV. Sortilin is essential and sufficient for the formation of Glut4 storage vesicles in 3T3-L1 adipocytes. Dev Cell. 2005; 9:99–108. [PubMed: 15992544]
21. Watson RT, Khan AH, Furukawa M, Hou JC, Li L, Kanzaki M, Okada S, Kandror KV, Pessin JE. Entry of newly synthesized GLUT4 into the insulin-responsive storage compartment is GGA dependent. EMBO J. 2004; 23:2059–2070. [PubMed: 15116067]
22. Huang G, Buckler-Pena D, Nauta T, Singh M, Asmar A, Shi J, Kim JY, Kandror KV. Insulin responsiveness of glucose transporter 4 in 3T3-L1 cells depends on the presence of sortilin. Mol Biol Cell. 2013; 24:3115–3122. [PubMed: 23966466]
23. Tsuchiya Y, Hatakeyama H, Emoto N, Wagatsuma F, Matsushita S, Kanzaki M. Palmitate-induced down-regulation of sortilin and impaired GLUT4 trafficking in C2C12 myotubes. J Biol Chem. 2010; 285:34371–34381. [PubMed: 20805226]
24. Kaddai V, Jager J, Gonzalez T, Najem-Lendom R, Bonnafous S, Tran A, Le Marchand-Brustel Y, Gual P, Tanti JF, Cormont M. Involvement of TNF-alpha in abnormal adipocyte and muscle sortilin expression in obese mice and humans. Diabetologia. 2009; 52:932–940. [PubMed: 19219422]
25. Rabinowich L, Fishman S, Hubel E, Thurm T, Park WJ, Pewzner-Jung Y, Saroha A, Erez N, Halpern Z, Futerman AH, Zvibel I. Sortilin deficiency improves the metabolic phenotype and reduces hepatic steatosis of mice subjected to diet-induced obesity. J Hepatol. 2015; 62:175–181. [PubMed: 25173968]
26. Steele R, Wall JS, De Bodo RC, Altszuler N. Measurement of size and turnover rate of body glucose pool by the isotope dilution method. The American journal of physiology. 1956; 187:15–24. [PubMed: 13362583]
27. Kraegen EW, James DE, Jenkins AB, Chisholm DJ. Dose-response curves for in vivo insulin sensitivity in individual tissues in rats. Am J Physiol. 1985; 248:E353–362. [PubMed: 3883806]
28. Turpin SM, Nicholls HT, Willmes DM, Mourier A, Brodesser S, Wunderlich CM, Mauer J, Xu E, Hammerschmidt P, Bronneke HS, Trifunovic A, LoSasso G, Wunderlich FT, Kornfeld JW, Bluher M, Kronke M, Bruning JC. Obesity-induced CerS6-dependent C16:0 ceramide production promotes weight gain and glucose intolerance. Cell Metab. 2014; 20:678–686. [PubMed: 25295788]
29. Raichur S, Wang ST, Chan PW, Li Y, Ching J, Chaurasia B, Dogra S, Ohman MK, Takeda K, Sugii S, Pewzner-Jung Y, Futerman AH, Summers SA. CerS2 haploinsufficiency inhibits beta-oxidation and confers susceptibility to diet-induced steatohepatitis and insulin resistance. Cell Metab. 2014; 20:687–695. [PubMed: 25295789]
30. Ni X, Morales CR. The lysosomal trafficking of acid sphingomyelinase is mediated by sortilin and mannose 6-phosphate receptor. Traffic. 2006; 7:889–902. [PubMed: 16787399]
31. Leto D, Saltiel AR. Regulation of glucose transport by insulin: traffic control of GLUT4. Nat Rev Mol Cell Biol. 2012; 13:383–396. [PubMed: 22617471]
32. Keller SR, Davis AC, Clairmont KB. Mice deficient in the insulin-regulated membrane aminopeptidase show substantial decreases in glucose transporter GLUT4 levels but maintain normal glucose homeostasis. The Journal of biological chemistry. 2002; 277:17677–17686. [PubMed: 11884418]
33. Jedrychowski MP, Gartner CA, Gygi SP, Zhou L, Herz J, Kandror KV, Pilch PF. Proteomic analysis of GLUT4 storage vesicles reveals LRP1 to be an important vesicle component and target of insulin signaling. J Biol Chem. 2010; 285:104–114. [PubMed: 19864425]
34. Kandror KV, Pilch PF. The insulin-like growth factor II/mannose 6-phosphate receptor utilizes the same membrane compartments as GLUT4 for insulin-dependent trafficking to and from the rat adipocyte cell surface. The Journal of biological chemistry. 1996; 271:21703–21708. [PubMed: 8702963]
35. Hou JC, Pessin JE. Ins (endocytosis) and outs (exocytosis) of GLUT4 trafficking. Current opinion in cell biology. 2007; 19:466–473. [PubMed: 17644329]
36. Katz EB, Stenbit AE, Hatton K, DePinho R, Charron MJ. Cardiac and adipose tissue abnormalities but not diabetes in mice deficient in GLUT4. Nature. 1995; 377:151–155. [PubMed: 7675081]
37. Bikman BT, Summers SA. Ceramides as modulators of cellular and whole-body metabolism. J Clin Invest. 2011; 121:4222–4230. [PubMed: 22045572]

38. Jansen P, Giehl K, Nyengaard JR, Teng K, Lioubinski O, Sjoegaard SS, Breiderhoff T, Gotthardt M, Lin F, Eilers A, Petersen CM, Lewin GR, Hempstead BL, Willnow TE, Nykjaer A. Roles for the pro-neurotrophin receptor sortilin in neuronal development, aging and brain injury. Nature neuroscience. 2007; 10:1449–1457. [PubMed: 17934455]

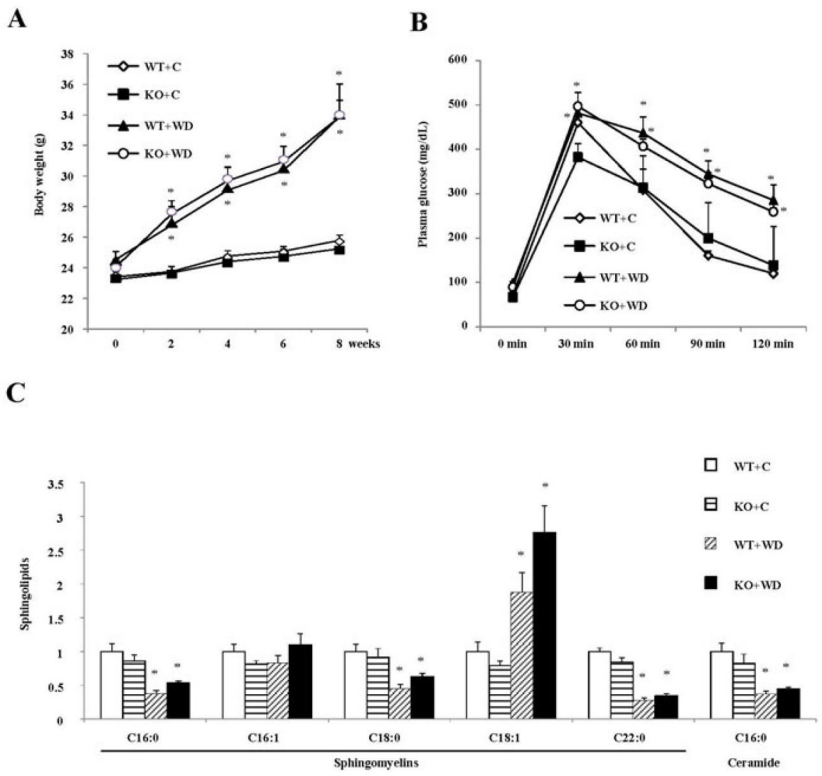

FIGURE 1. Sort1 knockout did not affect diet-induced obesity or adipose ceramide concentration in mice

Mice were fed a chow diet (C) or a Western diet (WD) for 8 week. Mice were fasted overnight before sacrifice. **A**. Body weight. (n=4–9). **B**. Glucose tolerance test. (n=4–9). **C**. Metabolites were measured in epididymal fat of mice fed a chow or a Western diet for 8 week. Mice were fasted overnight before sacrifice. Y-axis: relative area under the curve with control (WT+C) set as "1". n=4–6. All results are expressed as mean ± SEM. "*", $p < 0.05$. vs. WT+C group.

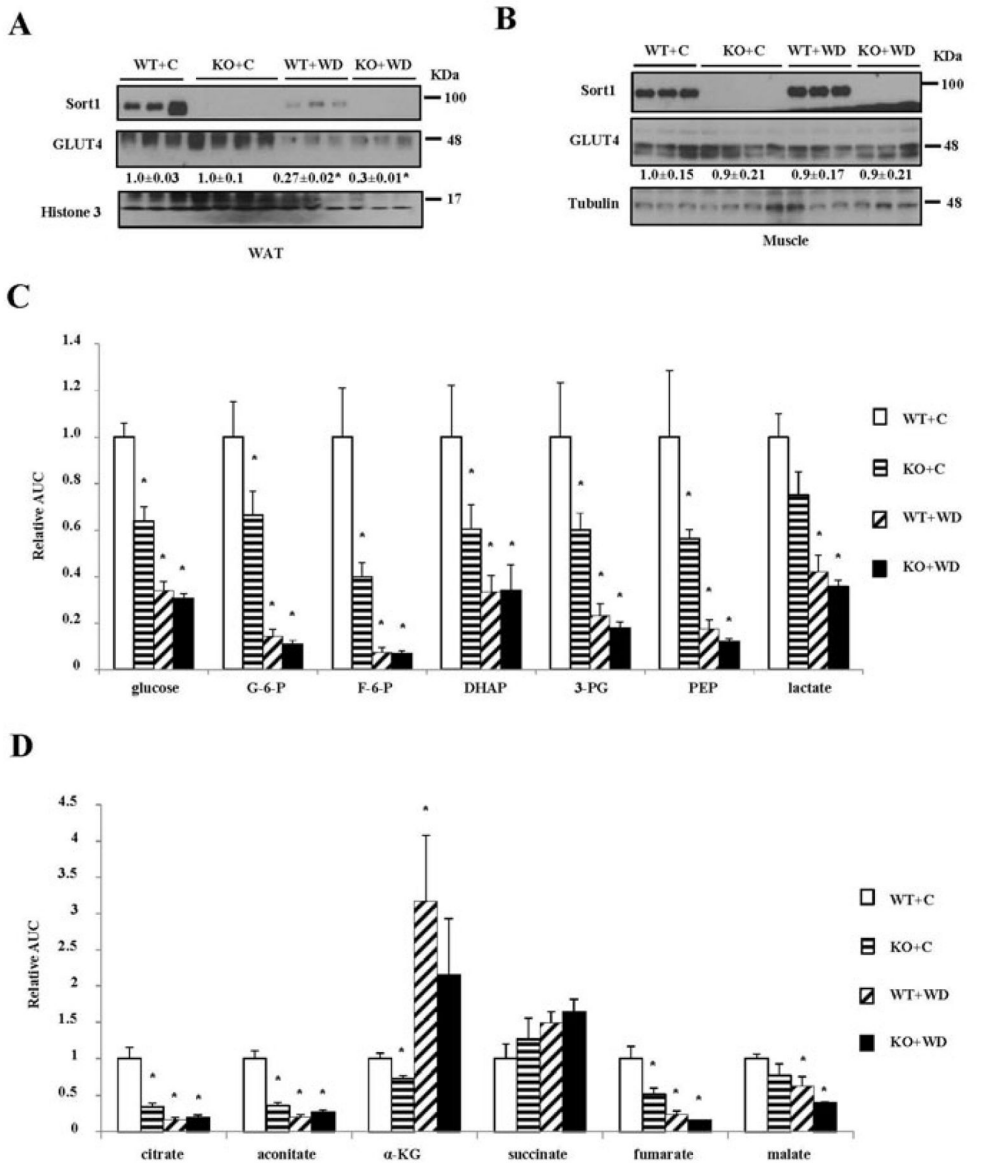

FIGURE 2. *Sort1* KO mice showed reduced adipose glycolytic and TCA cycle intermediates

Mice were fed a chow or a Western diet for 8 week. Mice were fasted overnight before sacrifice. **A**, **B**. Western blot of Sort1 and Glut4 protein in epididymal fat and soleus muscle of WT and *Sort1* KO mice fed a chow or a Western diet (WD). **C. D**. Relative concentrations of metabolites in the epididymal adipose tissue. Y-axis: relative area under the curve with control (WT+C) set as "1". n=4–6. Results are expressed as mean ± SEM. "*", $p < 0.05$. vs. WT+C group. G-6-P: glucose-6-phosphate; DHAP: dihydroxyacetone phosphate; 3-PG: glyceraldehyde 3-phosphate; PEP: phosphoenolpyruvate; α-KG: α-ketoglutarate.

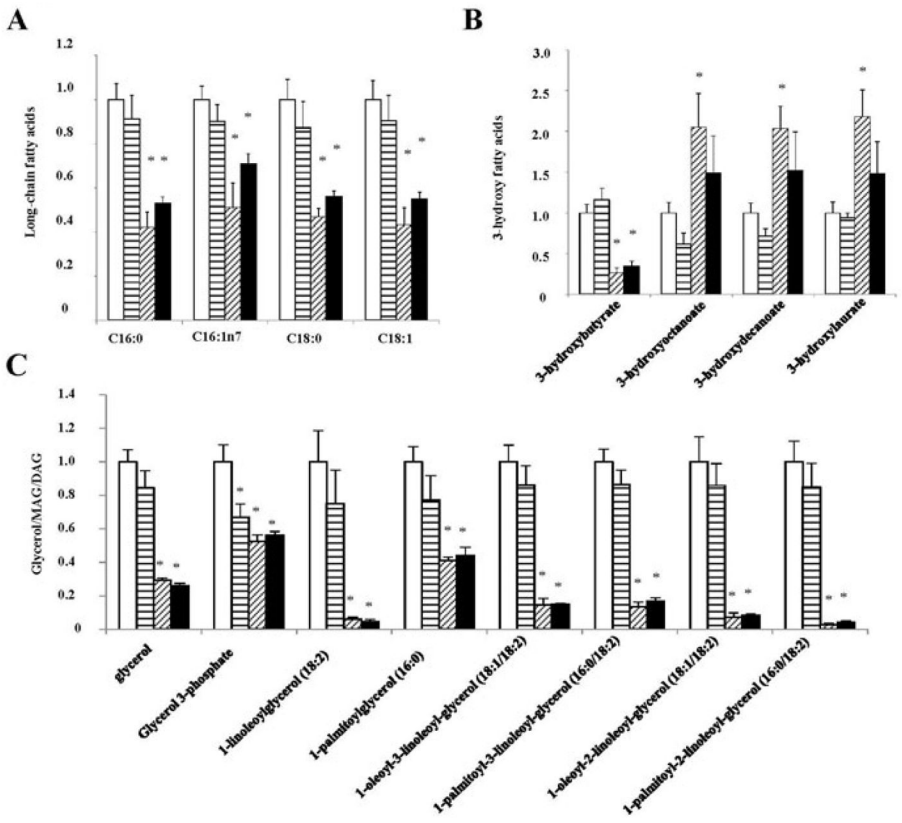

FIGURE 3. Sort1 knockout did not affect adipose fatty acid metabolism in mice

Mice were fed a chow or a Western diet for 8 week. Mice were fasted overnight before sacrifice. **A**. Long chain fatty acid species. **B**. 3-hydroxy fatty acids. **C**. Glycerol, glycerol 3-phosphate, monoacylglyerol (MAG) and diacylglycerol (DAG). Y-axis: relative area under the curve with control (WT+C) set as “1”. n=4–6. Results are expressed as mean ± SEM. “*”, $p < 0.05$. vs. WT+C group.

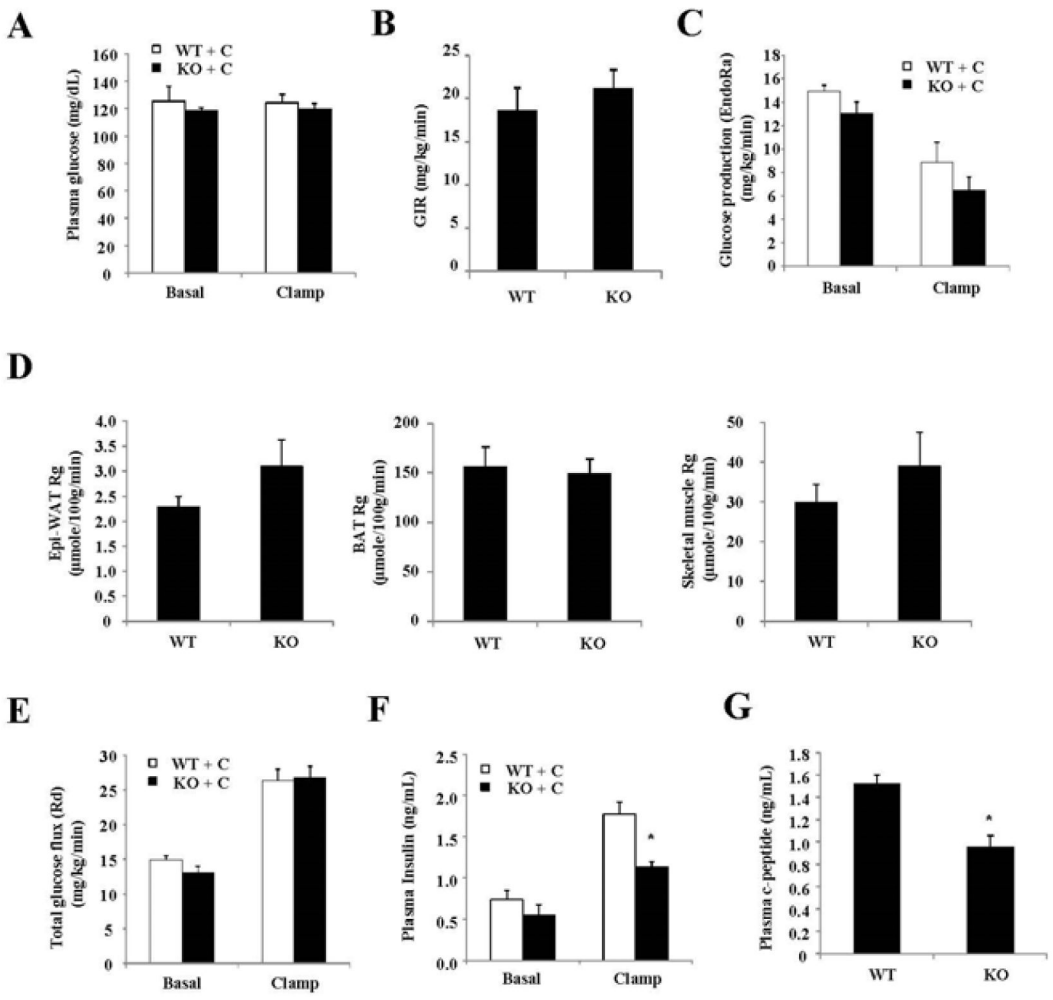

FIGURE 4. Hyperinsulinemic-euglycemic clamp study of chow-fed mice

The experimental procedure is described in the Materials and Method. Hyperinsulinemic-euglycemic clamp parameters. GIR: glucose infusion rate. Rg: tissue glucose uptake. Skeletal muscle: Soleus muscle. Epi-WAT: Epididymal fat. BAT: brown adipose tissue. (n=8). Results are expressed as mean ± SEM. "*", $p < 0.05$ vs. WT.

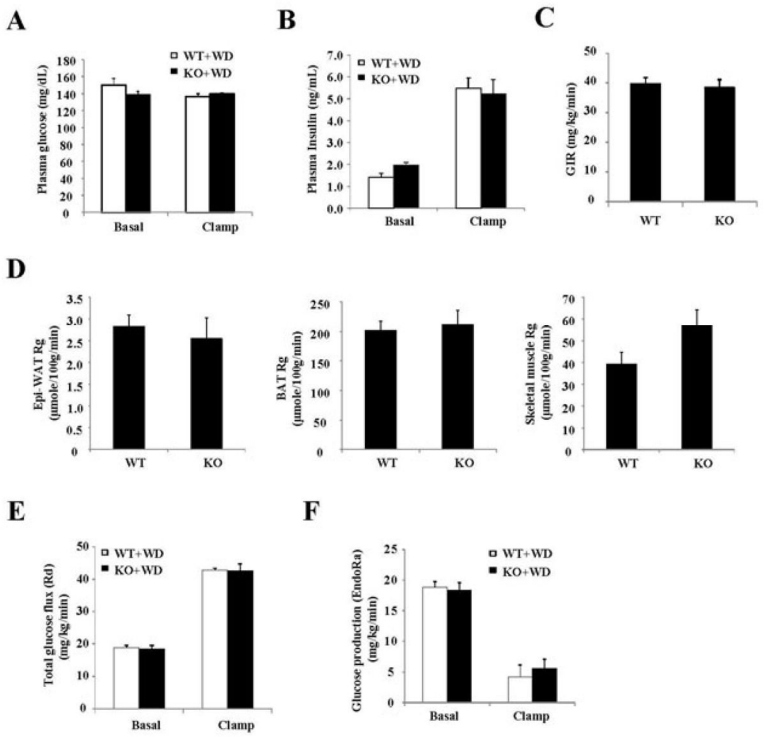

FIGURE 5. Hyperinsulinemic-euglycemic clamp study of 8-week Western diet-fed mice

The experimental procedure is described in the Materials and Method. Hyperinsulinemic-euglycemic clamp parameters. GIR: glucose infusion rate. Rg: tissue glucose uptake. Skeletal muscle: Soleus muscle. Epi-WAT: Epididymal fat. BAT: brown adipose tissue. n=8–9. Results are expressed as mean ± SEM.